IEEE Access
Multidisciplinary ⋮ Rapid Review ⋮ Open Access Journal

Received 8 March 2023, accepted 17 March 2023, date of publication 3 April 2023, date of current version 6 April 2023.

Digital Object Identifier 10.1109/ACCESS.2023.3263947

RESEARCH ARTICLE

Control of Prioritized and Separated Periodic/Aperiodic Task

HISAYOSHI MURAMATSU[1], (Member, IEEE), AND MASAKI HINO[2]
[1]Mechanical Engineering Program, Hiroshima University, Higashihiroshima, Hiroshima 739-8527, Japan
[2]Technical Division, Satake Corporation, Higashihiroshima, Hiroshima 739-8602, Japan

Corresponding author: Hisayoshi Muramatsu (muramatsu@hiroshima-u.ac.jp)

This work was supported by JST, ACT-X, Japan, under Grant JPMJAX200Q.

ABSTRACT Robots are typically expected to perform multiple tasks. For realizing multiple tasks using multi-degrees-of-freedom of a robot, priority control was developed. The priority control prioritizes conflicting tasks by projecting lower-priority task velocity into a null space of higher-priority task spaces. Similarly, for realizing two tasks on a single-degree-of-freedom of a robot, periodic/aperiodic separation control was developed. The periodic/aperiodic separation control separates a state into quasi-periodic and quasi-aperiodic states and feedback controls them separately. Thus, the priority control and periodic/aperiodic separation control realize multiple tasks in a different manner, and this paper proposes an integration of them to increase the number of simultaneously realized multiple tasks. Furthermore, this study analyzed the stability and conducted experiments to validate the proposed method. In the experiments, the proposed method achieved to increase the number of realizable tasks from six to nine by performing the quasi-periodic and quasi-aperiodic tasks in addition to prioritized tasks.

INDEX TERMS Priority control, periodic/aperiodic separation control, periodic/aperiodic separation filter, null space, redundant robot.

I. INTRODUCTION

Robots are typically required to perform multiple tasks simultaneously. For example, a pick-and-place task requires grasping an object, carrying it, and avoiding obstacles, simultaneously. To achieve such several tasks, hybrid control and priority control were proposed by utilizing multi-degrees-of-freedom of a robot, and periodic/aperiodic separation control was proposed for a single-degree-of-freedom of a robot.

The hybrid control can assign different control to each degree of freedom of a robot, where multiple tasks can be realized in different directions. Although the hybrid control can realize different tasks simultaneously, it cannot perform conflicting tasks. In contrast, the priority control can realize several conflicting tasks with prioritization, in which lower-priority tasks are prioritized to not disturb higher-priority tasks. The task priority control based on a null-space projection [1], [2], [3], [4], [5], [6], [7], [8], [9], [10] modifies task spaces of lower-priority tasks to be in null-space of higher-priority tasks, in which the lower-priority tasks are modified to not disturb the higher-priority tasks. Similarly, the task priority control based on hierarchical quadratic programming [11], [12], [13], [14] optimizes lower-priority task realization under satisfying higher-priority constraints. These priority controls can realize conflicting tasks with prioritization, while they cannot realize multiple tasks in the same priority level. Lastly, task priority control based on weighting [15], [16] can perform multiple tasks in the same priority level while conflicts among tasks occur. Therefore, despite the above advantages, the hybrid and priority controls cannot realize multiple controls separately on a single-degree-of-freedom.

The periodic/Aperiodic separation control was proposed to achieve quasi-periodic and quasi-aperiodic controls on a single-degree-of-freedom [17], [18], [19]. By using a periodic/aperiodic separation filter (PASF), a state is separated into quasi-periodic and quasi-aperiodic states, and the separated quasi-periodic and quasi-aperiodic tasks are simultaneously achieved. In contrast, the PASF is similar to comb filters including an infinite number of band stops, which are used for

The associate editor coordinating the review of this manuscript and approving it for publication was Okyay Kaynak.

the harmonics noise elimination [20], [21], [22] and periodic disturbance elimination [23], [24]. The PASF is composed of periodic-pass and aperiodic-pass filters, which separate a signal into quasi-periodic and quasi-aperiodic signals, and the aperiodic-pass filter can be regarded as a generalized comb filter because the aperiodic-pass filter is also capable of eliminating the harmonics. Compared to the comb filters, the cutoff frequency, convergence speed, and high-order filters of the first-order PASF can be easily adjusted [25].

To increase functions of a redundant robot, further increase in simultaneously realizable tasks is effective. To this end, this paper integrates the above priority control and periodic/aperiodic separation control and proposes periodic/aperiodic task priority control. The proposed method realizes multiple periodic/aperiodic tasks with prioritization based on a null space projection, and each periodic/aperiodic task can contain separated quasi-periodic and quasi-aperiodic tasks. The contributions of the paper are the number of simultaneously realized multiple tasks is increased by implementing the quasi-periodic and quasi-aperiodic tasks in the same priority level compared to the priority control, and the global asymptotic stability is proved for the system using the proposed method including time delay and nonlinear Jacobian matrices.

II. PRIORITIZATION OF TASKS

This section introduces tasks, prioritization of the tasks, and control of the prioritized task for a redundant robot. First, task coordinates and Jacobian matrices are defined, and their characteristics are shown. Then, the task velocities are changed into prioritized task velocities using the Jacobian matrices on the basis of the null projection. Lastly, torque input to a redundant robot is derived to control the prioritized tasks.

Consider an n-DOF redundant robot

$$\boldsymbol{M}\ddot{\boldsymbol{q}} = \boldsymbol{\tau}, \tag{1}$$

where $\boldsymbol{M} \in \mathbb{R}^{n\times n}$, $\boldsymbol{q} \in \mathrm{R}^n$, and $\boldsymbol{\tau} \in \mathrm{R}^n$ denote the moment of inertia, joint angle, and motor torque, respectively. We define task coordinates $\boldsymbol{x}i \in \mathbb{R}^{mi}$ and a mapping $\boldsymbol{\Phi}i : \mathbb{R}^n \to \mathbb{R}^{mi}$ from the joint space $\boldsymbol{q}$ to the task space $\boldsymbol{x}i \in \mathrm{R}^{mi}$

$$\boldsymbol{x}i := \boldsymbol{\Phi}i(\boldsymbol{q}). \tag{2}$$

Among the tasks, we assign priority to the tasks as $\boldsymbol{x}i$ is prior to $\boldsymbol{x}j$ if $i < j$, where the number of the tasks is assumed to be k. Then, the whole dimension matches the degrees of freedom n of the robot as

$$\sum i = 1^k mi = n. \tag{3}$$

For the task coordinates $\boldsymbol{x}i \in \mathrm{R}^{mi}$, joint angle $\boldsymbol{q} \in \mathrm{R}^n$, prioritized joint angles $\bar{\boldsymbol{q}}i \in \mathrm{R}^n$, and prioritized task coordinates $\bar{\boldsymbol{x}}i \in \mathrm{R}^{mi}$, Jacobian matrices are defined as

$$\boldsymbol{J}i := \frac{\partial \boldsymbol{x}i}{\partial \boldsymbol{q}} := \frac{\partial \bar{\boldsymbol{x}}i}{\partial \bar{\boldsymbol{q}}i} \in \mathbb{R}^{mi\times n} \tag{4a}$$

$$\boldsymbol{N}i := \frac{\partial \bar{\boldsymbol{q}}i}{\partial \boldsymbol{q}} \in \mathbb{R}^{n\times n}$$

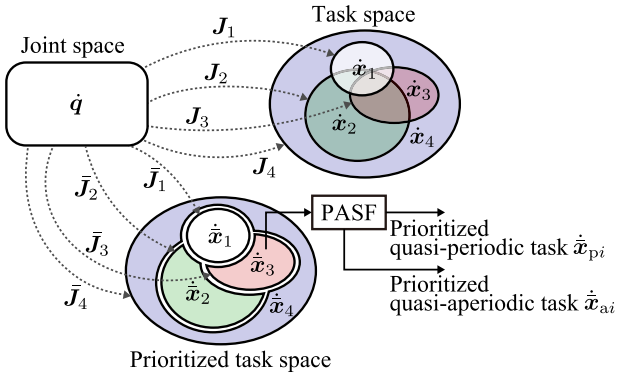

FIGURE 1. Conceptual diagram of the spaces.

$$:= \begin{cases} \boldsymbol{I} & \text{if } i = 1 \\ \boldsymbol{N}i - 1 - \bar{\boldsymbol{J}}i - 1^{+}\bar{\boldsymbol{J}}i - 1 & \text{if } i > 1. \end{cases} \tag{4b}$$

$$\bar{\boldsymbol{J}}i := \frac{\partial \bar{\boldsymbol{x}}i}{\partial \boldsymbol{q}} = \boldsymbol{J}i\boldsymbol{N}i \in \mathbb{R}^{mi\times n}, \tag{4c}$$

where $\boldsymbol{N}i$ is the null space projection matrix, and $\bar{\boldsymbol{J}}i^{+}$ is the generalized inverse matrix of $\bar{\boldsymbol{J}}i$

$$\bar{\boldsymbol{J}}i^{+} := \bar{\boldsymbol{J}}i^{\top}(\bar{\boldsymbol{J}}i\bar{\boldsymbol{J}}i^{\top})^{-1} \in \mathbb{R}^{n\times mi}. \tag{5}$$

Figure 1 illustrates the relationship among the spaces, in which the intersections of the task spaces are assigned to a higher-priority task by the prioritization. The Jacobian matrices satisfy

$$\bar{\boldsymbol{J}}i\bar{\boldsymbol{J}}j^{+} = \begin{cases} \boldsymbol{I} & \text{if } i = j \\ \boldsymbol{0} & \text{if } i \neq j \end{cases} \tag{6a}$$

$$\boldsymbol{J}i\bar{\boldsymbol{J}}j^{+} = \begin{cases} \boldsymbol{I} & \text{if } i = j \\ \boldsymbol{0} & \text{if } i < j \\ \boldsymbol{J}i\bar{\boldsymbol{J}}j^{+} & \text{if } i > j, \end{cases} \tag{6b}$$

which are derived below.

The matrix $\bar{\boldsymbol{J}}i^{+}\bar{\boldsymbol{J}}i$ is symmetric because $\bar{\boldsymbol{J}}i^{+}\bar{\boldsymbol{J}}i = \bar{\boldsymbol{J}}i^{\top}(\bar{\boldsymbol{J}}i\bar{\boldsymbol{J}}i^{\top})^{-1}\bar{\boldsymbol{J}}i$, where $(\bar{\boldsymbol{J}}i\bar{\boldsymbol{J}}i^{\top})^{-1}$ is also symmetric because $\bar{\boldsymbol{J}}i\bar{\boldsymbol{J}}i^{\top}$ is symmetric. Moreover, the null space projection matrix $\boldsymbol{N}i$ is symmetric because it is the sum of the symmetric matrices $\boldsymbol{N}i - 1$ and $\boldsymbol{J}i^{+}\boldsymbol{J}i$ as (4b). If $\boldsymbol{N}i^2 = \boldsymbol{N}i$,

$$\bar{\boldsymbol{J}}i\bar{\boldsymbol{J}}i^{+} = \bar{\boldsymbol{J}}i\bar{\boldsymbol{J}}i^{\top}(\bar{\boldsymbol{J}}i\bar{\boldsymbol{J}}i^{\top})^{-1} = \boldsymbol{I} \tag{7a}$$

$$\bar{\boldsymbol{J}}i\boldsymbol{N}i = \boldsymbol{J}i\boldsymbol{N}i^2 = \bar{\boldsymbol{J}}i \tag{7b}$$

$$\boldsymbol{N}i\bar{\boldsymbol{J}}i^{+} = \boldsymbol{N}i^2\boldsymbol{J}i^{\top}(\bar{\boldsymbol{J}}i\bar{\boldsymbol{J}}i^{\top})^{-1} = \bar{\boldsymbol{J}}i^{+}, \tag{7c}$$

which give

$$\begin{aligned} \boldsymbol{N}i + 1^2 &= (\boldsymbol{N}i - \bar{\boldsymbol{J}}i^{+}\bar{\boldsymbol{J}}i)^2 \\ &= \boldsymbol{N}i^2 - \boldsymbol{N}i\bar{\boldsymbol{J}}i^{+}\bar{\boldsymbol{J}}i - \bar{\boldsymbol{J}}i^{+}\bar{\boldsymbol{J}}i\boldsymbol{N}i + \bar{\boldsymbol{J}}i^{+}\bar{\boldsymbol{J}}i\bar{\boldsymbol{J}}i^{+}\bar{\boldsymbol{J}}i \\ &= \boldsymbol{N}i + 1. \end{aligned} \tag{8}$$

Thus, $\boldsymbol{N}i^2 = \boldsymbol{N}i \Rightarrow \boldsymbol{N}i + 1^2 = \boldsymbol{N}i + 1$. Because $\boldsymbol{N}1^2 = \boldsymbol{I}^2 = \boldsymbol{N}1$,

$$\boldsymbol{N}i^2 = \boldsymbol{N}i, \ \forall i \in \mathbb{Z}_{>} 0 \tag{9}$$

and (7) holds for $i \in \mathbb{Z}> 0$. Additionally, the multiplication of $\boldsymbol{N}i$ satisfies

$$\begin{aligned}\boldsymbol{N}i\boldsymbol{N}i+1 &= \boldsymbol{N}i^2 - \boldsymbol{N}i\bar{\boldsymbol{J}}i^+\bar{\boldsymbol{J}}i = \boldsymbol{N}i - \bar{\boldsymbol{J}}i^+\bar{\boldsymbol{J}}i \\ &= \boldsymbol{N}i+1,\ \forall i \in \mathbb{Z}> 0 \qquad (10a)\\ \boldsymbol{N}i &= \boldsymbol{N}i-1\boldsymbol{N}i = \boldsymbol{N}i-2\boldsymbol{N}i-1\boldsymbol{N}i = \cdots, \qquad (10b)\end{aligned}$$

and

$$\begin{aligned}\boldsymbol{N}i &= \boldsymbol{N}i^\top = (\boldsymbol{N}h\boldsymbol{N}h+1\cdots\boldsymbol{N}i)^\top \\ &= \boldsymbol{N}i\cdots\boldsymbol{N}h+1\boldsymbol{N}h,\ \forall h \in \{k \in \mathbb{Z}|0<k<i\}. \qquad (11)\end{aligned}$$

Moreover,

$$\begin{aligned}\boldsymbol{J}i\boldsymbol{N}i+1 &= \boldsymbol{J}i(\boldsymbol{N}i - \bar{\boldsymbol{J}}i^+\bar{\boldsymbol{J}}i) = \bar{\boldsymbol{J}}i - \boldsymbol{J}i\boldsymbol{N}i^2\boldsymbol{J}i^\top(\bar{\boldsymbol{J}}i\bar{\boldsymbol{J}}i^\top)^{-1}\bar{\boldsymbol{J}}i \\ &= \bar{\boldsymbol{J}}i - \bar{\boldsymbol{J}}i\bar{\boldsymbol{J}}i^\top(\bar{\boldsymbol{J}}i\bar{\boldsymbol{J}}i^\top)^{-1}\bar{\boldsymbol{J}}i = \boldsymbol{0}. \qquad (12)\end{aligned}$$

Consider (6a). If $i=j, \bar{\boldsymbol{J}}i\bar{\boldsymbol{J}}j^+ = \boldsymbol{I}$ according to (7). If $i<j$, using (11) and (12),

$$\begin{aligned}\bar{\boldsymbol{J}}i\bar{\boldsymbol{J}}j^+ &= \bar{\boldsymbol{J}}i\bar{\boldsymbol{J}}j^\top(\bar{\boldsymbol{J}}j\bar{\boldsymbol{J}}j^\top)^{-1} = \boldsymbol{J}i\boldsymbol{N}i\boldsymbol{N}j\boldsymbol{J}j^\top(\bar{\boldsymbol{J}}j\bar{\boldsymbol{J}}j^\top)^{-1} \\ &= \boldsymbol{J}i\boldsymbol{N}i\boldsymbol{N}i+1\cdots\boldsymbol{N}j\boldsymbol{J}j^\top(\bar{\boldsymbol{J}}j\bar{\boldsymbol{J}}j^\top)^{-1} \\ &= \boldsymbol{J}i\boldsymbol{N}i+1\cdots\boldsymbol{N}j\boldsymbol{J}j^\top(\bar{\boldsymbol{J}}j\bar{\boldsymbol{J}}j^\top)^{-1} = \boldsymbol{0}. \qquad (13)\end{aligned}$$

If $i>j$, using (11) and (12),

$$\begin{aligned}\bar{\boldsymbol{J}}i\bar{\boldsymbol{J}}j^+ &= \bar{\boldsymbol{J}}i\bar{\boldsymbol{J}}j^\top(\bar{\boldsymbol{J}}j\bar{\boldsymbol{J}}j^\top)^{-1} = \boldsymbol{J}i\boldsymbol{N}i\boldsymbol{N}j\boldsymbol{J}j^\top(\bar{\boldsymbol{J}}j\bar{\boldsymbol{J}}j^\top)^{-1} \\ &= \boldsymbol{J}i\boldsymbol{N}i\cdots\boldsymbol{N}j+1\boldsymbol{N}j\boldsymbol{J}j^\top(\bar{\boldsymbol{J}}j\bar{\boldsymbol{J}}j^\top)^{-1} \\ &= \boldsymbol{J}i\boldsymbol{N}i\cdots\boldsymbol{N}j+1\boldsymbol{J}j^\top(\bar{\boldsymbol{J}}j\bar{\boldsymbol{J}}j^\top)^{-1} = \boldsymbol{0}. \qquad (14)\end{aligned}$$

Therefore, (6a) holds. Consider (6b). If $i=j$, using (9),

$$\begin{aligned}\boldsymbol{J}i\bar{\boldsymbol{J}}j^+ &= \boldsymbol{J}i\boldsymbol{N}i\boldsymbol{J}i^\top(\bar{\boldsymbol{J}}i\bar{\boldsymbol{J}}i^\top)^{-1} = \boldsymbol{J}i\boldsymbol{N}i^2\boldsymbol{J}i^\top(\bar{\boldsymbol{J}}i\bar{\boldsymbol{J}}i^\top)^{-1} \\ &= \bar{\boldsymbol{J}}i\bar{\boldsymbol{J}}i^+ = \boldsymbol{I}. \qquad (15)\end{aligned}$$

If $i<j$, using (11) and (12),

$$\begin{aligned}\boldsymbol{J}i\bar{\boldsymbol{J}}j^+ &= \boldsymbol{J}i\boldsymbol{N}j\boldsymbol{J}j^\top(\bar{\boldsymbol{J}}j\bar{\boldsymbol{J}}j^\top)^{-1} \\ &= \boldsymbol{J}i\boldsymbol{N}i+1\cdots\boldsymbol{N}j\boldsymbol{J}j^\top(\bar{\boldsymbol{J}}j\bar{\boldsymbol{J}}j^\top)^{-1} = \boldsymbol{0}. \qquad (16)\end{aligned}$$

Therefore, (6b) holds.

We set the angular velocity as

$$\dot{\boldsymbol{q}} := \sum i = 1^k \bar{\boldsymbol{J}}i^+\dot{\boldsymbol{x}}i^{\mathrm{ref}}, \qquad (17)$$

where $\dot{\boldsymbol{x}}i^{\mathrm{ref}} \in \mathrm{R}^{mi}$ denotes the reference task velocity. Then, according to (6), it achieves

$$\begin{aligned}\dot{\boldsymbol{x}}i &= \boldsymbol{J}i\dot{\boldsymbol{q}} = \boldsymbol{J}i\sum j = 1^k \bar{\boldsymbol{J}}j^+\dot{\boldsymbol{x}}j^{\mathrm{ref}} \\ &= \dot{\boldsymbol{x}}i^{\mathrm{ref}} + \boldsymbol{J}i\sum j = 1^{i-1}\bar{\boldsymbol{J}}j^+\dot{\boldsymbol{x}}j^{\mathrm{ref}} \qquad (18a)\\ \dot{\bar{\boldsymbol{x}}}i &= \bar{\boldsymbol{J}}i\dot{\boldsymbol{q}} = \bar{\boldsymbol{J}}i\sum j = 1^k \bar{\boldsymbol{J}}j^+\dot{\boldsymbol{x}}j^{\mathrm{ref}} = \dot{\boldsymbol{x}}i^{\mathrm{ref}}, \qquad (18b)\end{aligned}$$

and (17) is rewritten as

$$\dot{\boldsymbol{q}} = \boldsymbol{\Gamma}^\dagger\dot{\boldsymbol{z}}^{\mathrm{ref}}, \qquad (19)$$

where

$$\begin{aligned}\boldsymbol{\Gamma}^\dagger &:= \left[\bar{\boldsymbol{J}}1^+ \cdots \bar{\boldsymbol{J}}k^+\right] \in \mathbb{R}^{n\times n} \qquad (20a)\\ \dot{\boldsymbol{z}}^{\mathrm{ref}} &:= \left[(\dot{\boldsymbol{x}}1^{\mathrm{ref}})^\top \cdots (\dot{\boldsymbol{x}}k^{\mathrm{ref}})^\top\right]^\top \in \mathbb{R}^n. \qquad (20b)\end{aligned}$$

Accordingly, the angular acceleration can be calculated as

$$\ddot{\boldsymbol{q}} = \boldsymbol{\Gamma}^\dagger\ddot{\boldsymbol{z}}^{\mathrm{ref}} + \dot{\boldsymbol{\Gamma}}^\dagger\dot{\boldsymbol{z}}^{\mathrm{ref}} = \boldsymbol{\Gamma}^\dagger\ddot{\boldsymbol{z}}^{\mathrm{ref}} + \dot{\boldsymbol{\Gamma}}^\dagger\boldsymbol{\Gamma}\dot{\boldsymbol{q}}, \qquad (21)$$

where

$$\boldsymbol{\Gamma} := \left[\bar{\boldsymbol{J}}1^\top \cdots \bar{\boldsymbol{J}}k^\top\right]^\top \in \mathbb{R}^{n\times n} \qquad (22)$$

and $\boldsymbol{\Gamma}\boldsymbol{\Gamma}^\dagger = \boldsymbol{I}$ based on (6a). Consequently, the motor torque τ is obtained as

$$\boldsymbol{\tau} = \bar{\boldsymbol{M}}\ddot{\boldsymbol{z}}^{\mathrm{ref}} + \bar{\boldsymbol{C}}\dot{\boldsymbol{q}} \in \mathbb{R}^n, \qquad (23)$$

where

$$\bar{\boldsymbol{M}} := \boldsymbol{M}\boldsymbol{\Gamma}^\dagger \in \mathbb{R}^{n\times n},\ \bar{\boldsymbol{C}} := \boldsymbol{M}\dot{\boldsymbol{\Gamma}}^\dagger\boldsymbol{\Gamma} \in \mathbb{R}^{n\times n}. \qquad (24)$$

III. PERIODIC/APERIODIC SEPARATION OF TASKS

Section II formulated the priority control, while it was still unable to realize several tasks on a single priority level. This section introduces quasi-periodic and quasi-aperiodic tasks to double the number of realizable tasks in a single priority level.

We separate the prioritized task coordinate $\bar{z} = [\bar{\boldsymbol{x}}1^\top \cdots \bar{\boldsymbol{x}}k^\top]^\top$ into a quasi-periodic prioritized task coordinate $\bar{z}\mathrm{p} \in \mathbb{R}^n$ and quasi-aperiodic prioritized task coordinate $\bar{z}\mathrm{a} \in \mathbb{R}^n$ as

$$\begin{aligned}\mathcal{L}[\bar{z}\mathrm{p}] &:= F\mathrm{p}(s)\mathcal{L}[\bar{z}] \qquad (25a)\\ \mathcal{L}[\bar{z}\mathrm{a}] &:= F\mathrm{a}(s)\mathcal{L}[\bar{z}], \qquad (25b)\end{aligned}$$

where $F\mathrm{p}(s)$ and $F\mathrm{a}(s)$ are the periodic-pass and aperiodic-pass filters of the PASF, respectively. In a first-order case, the periodic-pass and aperiodic-pass filters of the first-order PASF are

$$\begin{aligned}F\mathrm{p}(s) &:= \frac{\rho\Pi(1+e^{-\Pi s})}{(\rho\Pi+2)+(\rho\Pi-2)e^{-\Pi s}} \qquad (26a)\\ F\mathrm{a}(s) &:= \frac{2(1-e^{-\Pi s})}{(\rho\Pi+2)+(\rho\Pi-2)e^{-\Pi s}}, \qquad (26b)\end{aligned}$$

and their continuous-time representation is

$$\begin{aligned}\bar{z}\mathrm{p}(t) &= p1\bar{z}\mathrm{p}(t-\Pi) + p2\bar{z}(t) + p2\bar{z}(t-\Pi) \qquad (27a)\\ \bar{z}\mathrm{a}(t) &= \bar{z}(t) - \bar{z}\mathrm{p}(t), \qquad (27b)\end{aligned}$$

where

$$p1 := \frac{2-\rho\Pi}{2+\rho\Pi},\ p2 := \frac{\rho\Pi}{2+\rho\Pi}. \qquad (28)$$

The Bode plots of the periodic-pass filer $F\mathrm{p}(s)$ and the aperiodic-pass filter $F\mathrm{a}(s)$ are depicted in Figure 2. The periodic-pass filter passes constant element and harmonics corresponding to the Fourier series $a0/2 + \sum n = 1^\infty an\cos(n\omega 0t) + bn\sin(n\omega 0t)$ and surrounding waves. Additionally, the aperiodic-pass filter is complementary to the periodic-pass filter and passes the other waves.

To control the quasi-periodic prioritized task coordinate $\bar{z}\mathrm{p}$ and quasi-aperiodic prioritized task coordinate $\bar{z}\mathrm{a}$, a proportional-derivative controller is used to compute the acceleration reference $\ddot{\boldsymbol{z}}^{\mathrm{ref}}$ of (23) with the quasi-periodic task

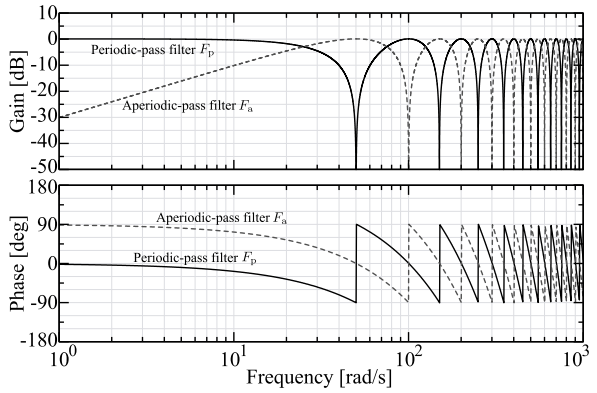

FIGURE 2. Bode plots of the periodic-pass filer Fp(s) and the aperiodic-pass filter Fa(s) of the PASF.

command $z\mathrm{p}^{\mathrm{cmd}} \in \mathbb{R}^n$ and quasi-aperiodic task command $z\mathrm{a}^{\mathrm{cmd}} \in \mathbb{R}^n$ as

$$\ddot{z}^{\mathrm{ref}} := \ddot{z}\mathrm{p}^{\mathrm{ref}} + \ddot{z}\mathrm{a}^{\mathrm{ref}} \tag{29a}$$
$$\ddot{z}\mathrm{p}^{\mathrm{ref}} := \boldsymbol{K}\mathrm{pp}(z\mathrm{p}^{\mathrm{cmd}} - \bar{z}\mathrm{p}) + \boldsymbol{K}\mathrm{pv}(\dot{z}\mathrm{p}^{\mathrm{cmd}} - \dot{\bar{z}}\mathrm{p}) \tag{29b}$$
$$\ddot{z}\mathrm{a}^{\mathrm{ref}} := \boldsymbol{K}\mathrm{ap}(z\mathrm{a}^{\mathrm{cmd}} - \bar{z}\mathrm{a}) + \boldsymbol{K}\mathrm{av}(\dot{z}\mathrm{a}^{\mathrm{cmd}} - \dot{\bar{z}}\mathrm{a}), \tag{29c}$$

where the diagonal gain matrices are as follows

$$\boldsymbol{K}\mathrm{pp} := \mathrm{diag}(K\mathrm{pp}1, \ \ldots, \ K\mathrm{pp}n) \in \mathbb{R}^{n\times n} \tag{30a}$$
$$\boldsymbol{K}\mathrm{pv} := \mathrm{diag}(K\mathrm{pv}1, \ \ldots, \ K\mathrm{pv}n) \in \mathbb{R}^{n\times n} \tag{30b}$$
$$\boldsymbol{K}\mathrm{ap} := \mathrm{diag}(K\mathrm{ap}1, \ \ldots, \ K\mathrm{ap}n) \in \mathbb{R}^{n\times n} \tag{30c}$$
$$\boldsymbol{K}\mathrm{av} := \mathrm{diag}(K\mathrm{av}1, \ \ldots, \ K\mathrm{av}n) \in \mathbb{R}^{n\times n}. \tag{30d}$$

The elements of $\bar{z} = [\bar{x}1^\top \ \cdots \ \bar{x}k^\top]^\top$ can be computed according to (18) as

$$\bar{x}i = xi - \int 0^t \boldsymbol{J}i \sum j = 1^{i-1} \bar{\boldsymbol{J}}j^+ \dot{\bar{x}}jd\tau, \tag{31}$$

and $\dot{\bar{z}}$ can be obtained as

$$\dot{\bar{z}} = \boldsymbol{\Gamma}\dot{\boldsymbol{q}}. \tag{32}$$

The block diagram of the proposed periodic/aperiodic task priority control is shown in Figure 3.

We consider the state-space representation of the periodic/aperiodic task priority control system. According to (18b), the reference and prioritized task velocities are equal

$$\dot{\bar{z}} := \left[\dot{\bar{x}}1^\top \ \cdots \ \dot{\bar{x}}k^\top\right]^\top = \dot{z}^{\mathrm{ref}}, \tag{33}$$

and the controller (29) can be transformed into

$$\ddot{\bar{z}} := \ddot{\bar{z}}\mathrm{p} + \ddot{\bar{z}}\mathrm{a} \tag{34a}$$
$$\ddot{\bar{z}}\mathrm{p} := \boldsymbol{K}\mathrm{pp}(z\mathrm{p}^{\mathrm{cmd}} - \bar{z}\mathrm{p}) + \boldsymbol{K}\mathrm{pv}(\dot{z}\mathrm{p}^{\mathrm{cmd}} - \dot{\bar{z}}\mathrm{p}) \tag{34b}$$
$$\ddot{\bar{z}}\mathrm{a} := \boldsymbol{K}\mathrm{ap}(z\mathrm{a}^{\mathrm{cmd}} - \bar{z}\mathrm{a}) + \boldsymbol{K}\mathrm{av}(\dot{z}\mathrm{a}^{\mathrm{cmd}} - \dot{\bar{z}}\mathrm{a}). \tag{34c}$$

Consequently, the state-space representation of the system is

$$\dot{\boldsymbol{\xi}}(t) = \boldsymbol{A}\boldsymbol{\xi}(t) + \boldsymbol{A}\mathrm{p}\boldsymbol{\xi}\mathrm{p}(t) + \boldsymbol{B}\boldsymbol{\eta}(t) \tag{35a}$$
$$\boldsymbol{\xi}\mathrm{p}(t) = p1\boldsymbol{\xi}\mathrm{p}(t-\Pi) + p2\boldsymbol{\xi}(t) + p2\boldsymbol{\xi}(t-\Pi), \tag{35b}$$

where

$$\boldsymbol{\xi} := \begin{bmatrix} \bar{z} \\ \dot{\bar{z}} \end{bmatrix} \in \mathbb{R}^{2n}, \ \boldsymbol{\xi}\mathrm{p} := \begin{bmatrix} \bar{z}\mathrm{p} \\ \dot{\bar{z}}\mathrm{p} \end{bmatrix} \in \mathbb{R}^{2n} \tag{36a}$$
$$\boldsymbol{\eta} := \begin{bmatrix} z\mathrm{p}^{\mathrm{cmd}} \\ \dot{z}\mathrm{p}^{\mathrm{cmd}} \\ z\mathrm{a}^{\mathrm{cmd}} \\ \dot{z}\mathrm{a}^{\mathrm{cmd}} \end{bmatrix} \in \mathbb{R}^{4n} \tag{36b}$$
$$\boldsymbol{A} := \begin{bmatrix} \boldsymbol{0} & \boldsymbol{I} \\ -\boldsymbol{K}\mathrm{ap} & -\boldsymbol{K}\mathrm{av} \end{bmatrix} \in \mathbb{R}^{2n\times 2n} \tag{36c}$$
$$\boldsymbol{A}\mathrm{p} := \begin{bmatrix} \boldsymbol{0} & \boldsymbol{0} \\ \boldsymbol{K}\mathrm{ap} - \boldsymbol{K}\mathrm{pp} & \boldsymbol{K}\mathrm{av} - \boldsymbol{K}\mathrm{pv} \end{bmatrix} \in \mathbb{R}^{2n\times 2n} \tag{36d}$$
$$\boldsymbol{B} := \begin{bmatrix} \boldsymbol{0} & \boldsymbol{0} & \boldsymbol{0} & \boldsymbol{0} \\ \boldsymbol{K}\mathrm{pp} & \boldsymbol{K}\mathrm{pv} & \boldsymbol{K}\mathrm{ap} & \boldsymbol{K}\mathrm{av} \end{bmatrix} \in \mathbb{R}^{2n\times 4n}. \tag{36e}$$

IV. STABILITY ANALYSIS

To support stable and convergent behavior of the state of the redundant robot with the proposed method, Theorem 1 shows the global asymptotic stability of the origin for the system (35).

Theorem 1: Consider the system (35) and zero commands: $z\mathrm{p}^{\mathrm{cmd}} = \boldsymbol{0}$, $\dot{z}\mathrm{p}^{\mathrm{cmd}} = \boldsymbol{0}$, $z\mathrm{a}^{\mathrm{cmd}} = \boldsymbol{0}$, and $\dot{z}\mathrm{a}^{\mathrm{cmd}} = \boldsymbol{0}$. If the matrix $\boldsymbol{A} + p2\boldsymbol{A}\mathrm{p}$ is Hurwitz, the origin $[\boldsymbol{\xi}^\top(t), \ \boldsymbol{\xi}^\top(t-\Pi), \ \boldsymbol{\xi}\mathrm{p}^\top(t-\Pi)] = \boldsymbol{0}$ is globally asymptotically stable.

Proof. As preliminaries, the system (35) can be expressed as

$$\dot{\boldsymbol{\xi}}(t) = \boldsymbol{A}\boldsymbol{\xi}(t) + \boldsymbol{A}\mathrm{p}\boldsymbol{\xi}\mathrm{p}(t) \tag{37a}$$
$$\boldsymbol{\xi}\mathrm{p}(t) = p1\boldsymbol{\xi}\mathrm{p}(t-\Pi) + p2\boldsymbol{\xi}(t) + p2\boldsymbol{\xi}(t-\Pi) \tag{37b}$$

under the zero commands: $z\mathrm{p}^{\mathrm{cmd}} = \boldsymbol{0}, \dot{z}\mathrm{p}^{\mathrm{cmd}} = \boldsymbol{0}, z\mathrm{a}^{\mathrm{cmd}} = \boldsymbol{0}$, and $\dot{z}\mathrm{a}^{\mathrm{cmd}} = \boldsymbol{0}$, which is equivalent to $\boldsymbol{\eta} = \boldsymbol{0}$. Besides, since the matrix $\boldsymbol{A} + p2\boldsymbol{A}\mathrm{p}$ is Hurwitz, given any symmetric positive definite matrix $\boldsymbol{Q} \succ 0$, there exists a unique symmetric positive definite matrix $\boldsymbol{P} \succ 0$ satisfying the Lyapunov equation:

$$(\boldsymbol{A} + p2\boldsymbol{A}\mathrm{p})^\top \boldsymbol{P} + \boldsymbol{P}(\boldsymbol{A} + p2\boldsymbol{A}\mathrm{p}) + \boldsymbol{Q} = \boldsymbol{0}. \tag{38}$$

Lastly, the matrix $\boldsymbol{A}\mathrm{p}^\top \boldsymbol{A}\mathrm{p}$ is positive semi-definite $\boldsymbol{A}\mathrm{p}^\top \boldsymbol{A}\mathrm{p} \succeq 0$ because

$$\boldsymbol{y}^\top \boldsymbol{A}\mathrm{p}^\top \boldsymbol{A}\mathrm{p}\boldsymbol{y} = \|\boldsymbol{A}\mathrm{p}\boldsymbol{y}\|^2 \geq 0, \ \forall \boldsymbol{y} \in \mathbb{R}^{2n}. \tag{39}$$

Consider the Lyapunov function candidate:

$$V := \boldsymbol{\xi}^\top \boldsymbol{P}\boldsymbol{\xi} + r \int t - \Pi^t \boldsymbol{\xi}^\top(\sigma)\boldsymbol{\xi}(\sigma)d\sigma + w \int t - \Pi^t \boldsymbol{\xi}\mathrm{p}^\top(\sigma)\boldsymbol{\xi}\mathrm{p}(\sigma)d\sigma, \tag{40}$$

such that

$$\lambda\mathrm{min}(\boldsymbol{Q}) > \sqrt{3\psi 1 + 3p2^2\psi 2} \tag{41a}$$
$$r := \psi 1/\lambda\mathrm{min}(\boldsymbol{Q}), \ w := \psi 2/\lambda\mathrm{min}(\boldsymbol{Q}) \tag{41b}$$
$$\psi 1 \in \{\psi \in \mathbb{R} > 0 | \psi > 3\gamma p2^2 + p2^2\psi 2\} \tag{41c}$$
$$\psi 2 \in \{\psi \in \mathbb{R} > 0 | \psi > 3\gamma p1^2/\alpha\} \tag{41d}$$
$$\gamma := \lambda\mathrm{max}^2(\boldsymbol{P})\lambda\mathrm{max}(\boldsymbol{A}\mathrm{p}^\top \boldsymbol{A}\mathrm{p}), \ \alpha := 1 - p1^2, \tag{41e}$$

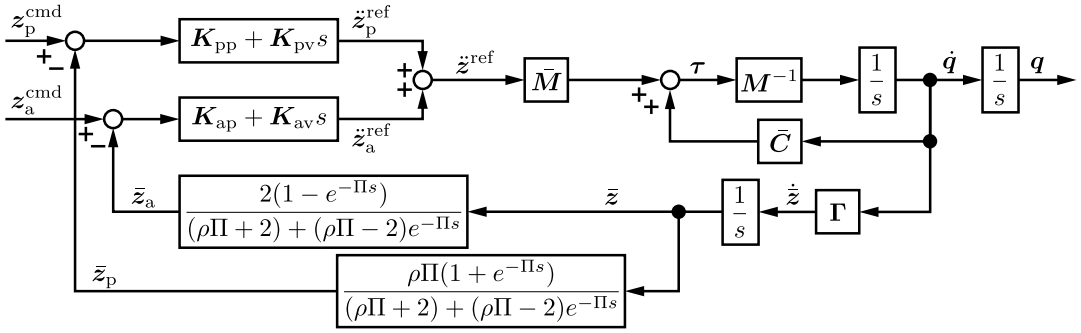

FIGURE 3. Block diagram of the proposed periodic/aperiodic task priority control.

where $\lambda\min(\boldsymbol{Q})$, r, w, $\psi 1$, $\psi 2$, $\alpha > 0$ and $\gamma \geq 0$. By substituting (37b) for (37a), the dynamics of $\boldsymbol{\xi}$ are

$$\begin{aligned}\dot{\boldsymbol{\xi}} &= (\boldsymbol{A}+p2\boldsymbol{A}\mathrm{p})\boldsymbol{\xi} \\ &\quad +p2\boldsymbol{A}\mathrm{p}\boldsymbol{\xi}(t-\Pi)+p1\boldsymbol{A}\mathrm{p}\boldsymbol{\xi}\mathrm{p}(t-\Pi). \end{aligned} \tag{42}$$

Hence, using (38), the derivative of the Lyapunov function candidate is

$$\begin{aligned}\dot{V} &= -\boldsymbol{\xi}^\top\boldsymbol{Q}\boldsymbol{\xi}+2\boldsymbol{\xi}^\top\boldsymbol{P}\boldsymbol{A}\mathrm{p}(p1\boldsymbol{\xi}\mathrm{p}(t-\Pi)+p2\boldsymbol{\xi}(t-\Pi)) \\ &\quad +r\|\boldsymbol{\xi}\|^2-r\|\boldsymbol{\xi}(t-\Pi)\|^2 \\ &\quad +w\|\boldsymbol{\xi}\mathrm{p}\|^2-w\|\boldsymbol{\xi}\mathrm{p}(t-\Pi)\|^2. \end{aligned} \tag{43}$$

Its terms are bounded as follows

$$\begin{aligned}&-\frac{2}{3}\boldsymbol{\xi}^\top\boldsymbol{Q}\boldsymbol{\xi}+2\boldsymbol{\xi}^\top\boldsymbol{P}\boldsymbol{A}\mathrm{p}(p1\boldsymbol{\xi}\mathrm{p}(t-\Pi)+p2\boldsymbol{\xi}(t-\Pi)) \\ &\quad\leq -\frac{1}{3}\left\|\sqrt{\lambda\min(\boldsymbol{Q})}\boldsymbol{\xi}-\frac{3p1}{\sqrt{\lambda\min(\boldsymbol{Q})}}\boldsymbol{P}\boldsymbol{A}\mathrm{p}\boldsymbol{\xi}\mathrm{p}(t-\Pi)\right\|^2 \\ &\qquad+\frac{3p1^2}{\lambda\min(\boldsymbol{Q})}\|\boldsymbol{P}\boldsymbol{A}\mathrm{p}\boldsymbol{\xi}\mathrm{p}(t-\Pi)\|^2 \\ &\qquad-\frac{1}{3}\left\|\sqrt{\lambda\min(\boldsymbol{Q})}\boldsymbol{\xi}-\frac{3p2}{\sqrt{\lambda\min(\boldsymbol{Q})}}\boldsymbol{P}\boldsymbol{A}\mathrm{p}\boldsymbol{\xi}(t-\Pi)\right\|^2 \\ &\qquad+\frac{3p2^2}{\lambda\min(\boldsymbol{Q})}\|\boldsymbol{P}\boldsymbol{A}\mathrm{p}\boldsymbol{\xi}(t-\Pi)\|^2 \\ &\quad\leq \frac{3\gamma p1^2}{\lambda\min(\boldsymbol{Q})}\|\boldsymbol{\xi}\mathrm{p}(t-\Pi)\|^2+\frac{3\gamma p2^2}{\lambda\min(\boldsymbol{Q})}\|\boldsymbol{\xi}(t-\Pi)\|^2, \end{aligned} \tag{44}$$

and

$$\begin{aligned}&\|\boldsymbol{\xi}\mathrm{p}\|^2-\|\boldsymbol{\xi}\mathrm{p}(t-\Pi)\|^2 \\ &\quad\leq \|p1\boldsymbol{\xi}\mathrm{p}(t-\Pi)+p2\boldsymbol{\xi}+p2\boldsymbol{\xi}(t-\Pi)\|^2-\|\boldsymbol{\xi}\mathrm{p}(t-\Pi)\|^2 \\ &\quad\leq -\alpha\|\boldsymbol{\xi}\mathrm{p}(t-\Pi)\|^2+p2^2\|\boldsymbol{\xi}\|^2+p2^2\|\boldsymbol{\xi}(t-\Pi)\|^2. \end{aligned} \tag{45}$$

From (44) and (45), the derivative is bounded as

$$\begin{aligned}\dot{V} &\leq -\left(\frac{1}{3}\lambda\min(\boldsymbol{Q})-r-wp2^2\right)\|\boldsymbol{\xi}\|^2 \\ &\quad-\left(r-\frac{3\gamma p2^2}{\lambda\min(\boldsymbol{Q})}-wp2^2\right)\|\boldsymbol{\xi}(t-\Pi)\|^2 \\ &\quad-\left(w\alpha-\frac{3\gamma p1^2}{\lambda\min(\boldsymbol{Q})}\right)\|\boldsymbol{\xi}\mathrm{p}(t-\Pi)\|^2. \end{aligned} \tag{46}$$

Owing to (41),

$$\begin{aligned}\frac{1}{3}\lambda\min(\boldsymbol{Q})-r-wp2^2 &= \frac{\lambda\min^2(\boldsymbol{Q})-3\psi 1-3p2^2\psi 2}{3\lambda\min(\boldsymbol{Q})} \\ &> 0 \end{aligned} \tag{47a}$$

$$\begin{aligned}r-\frac{3\gamma p2^2}{\lambda\min(\boldsymbol{Q})}-wp2^2 &= \frac{\psi 1-3\gamma p2^2-p2^2\psi 2}{\lambda\min(\boldsymbol{Q})} \\ &> 0 \end{aligned} \tag{47b}$$

$$w\alpha-\frac{3\gamma p1^2}{\lambda\min(\boldsymbol{Q})} = \frac{\alpha(\psi 2-3\gamma p1^2/\alpha)}{\lambda\min(\boldsymbol{Q})} > 0. \tag{47c}$$

Hence, the derivative $\dot{V}$ is zero at the origin and negative in the other region

$$\dot{V} = 0 \text{ if } \boldsymbol{\xi}(t)=\boldsymbol{\xi}(t-\Pi)=\boldsymbol{\xi}\mathrm{p}(t-\Pi)=\boldsymbol{0} \tag{48a}$$

$$\dot{V} < 0 \text{ otherwise.} \tag{48b}$$

Therefore, if the matrix $\boldsymbol{A}+p2\boldsymbol{A}\mathrm{p}$ is Hurwitz, the origin $[\boldsymbol{\xi}^\top(t),\ \boldsymbol{\xi}^\top(t-\Pi),\ \boldsymbol{\xi}\mathrm{p}^\top(t-\Pi)] = \boldsymbol{0}$ is globally asymptotically stable.

■

V. EXPERIMENTS

To validate that the proposed method increases the number of realizable tasks, we conducted experiments of the first-priority ball grasping task and the second-priority quasi-periodic positioning and quasi-aperiodic impedance control with the six degrees-of-freedom robot, as shown in Figure 4. The robot consisted of the upper and lower robots, and each robot had the two direct-drive motors for x and y movements and the linear motor for the z movement. The controllers were implemented on a PC with Linux and RTAI, where the sampling time was $T = 0.1 \times 10^{-3}$ s.

For the proposed periodic/aperiodic task priority control, the state, tasks, and Jacobian matrices were set as follows. The state $\boldsymbol{q}$ in the joint space was

$$\boldsymbol{q} = \left[\theta 1\ \theta 2\ z1\ \theta 3\ \theta 4\ z2\right]^\top, \tag{49}$$

and the coordinate of the first task $\boldsymbol{x}1$, that of the second quasi-periodic task $\boldsymbol{x}2\mathrm{p}$, and that of the second quasi-aperiodic task $\boldsymbol{x}2\mathrm{a}$ were

$$\boldsymbol{x}1 = \left[x1-x2\ y1-y2\ z1-z2\right]^\top \tag{50a}$$

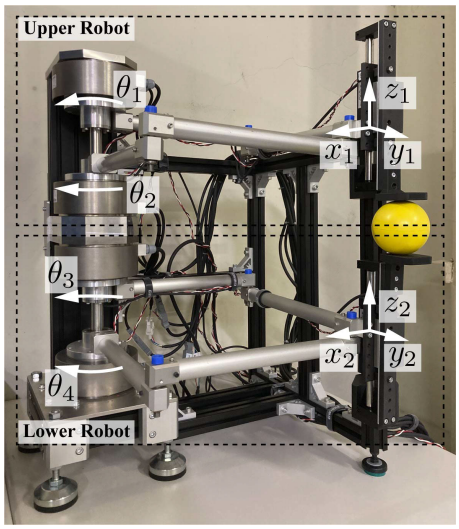

FIGURE 4. Experimental robot grasping a yellow ball.

$$\boldsymbol{x}2\mathrm{p} = \begin{bmatrix} x1\mathrm{p} & y1\mathrm{p} & z1\mathrm{p} \end{bmatrix}^\top \tag{50b}$$

$$\boldsymbol{x}2\mathrm{a} = \begin{bmatrix} x1\mathrm{a} & y1\mathrm{a} & z1\mathrm{a} \end{bmatrix}^\top. \tag{50c}$$

Accordingly, the matrices $\bar{\boldsymbol{M}}$ and $\bar{\boldsymbol{C}}$ of the controller (23) were based on the following Jacobian matrices

$$\boldsymbol{J}1 = [\boldsymbol{\Psi}(\theta 1, \theta 2) \quad -\boldsymbol{\Psi}(\theta 3, \theta 4)] \tag{51a}$$

$$\boldsymbol{J}2 = [\boldsymbol{\Psi}(\theta 1, \theta 2) \ \ \boldsymbol{0}], \tag{51b}$$

$$\boldsymbol{\Psi}(\psi 1, \ \psi 2) := \begin{bmatrix} -0.3\sin\psi 1 & -0.3\cos\psi 2 & 0 \\ 0.3\cos\psi 1 & -0.3\sin\psi 2 & 0 \\ 0 & 0 & 1 \end{bmatrix} \tag{51c}$$

$$\boldsymbol{N}1 = \boldsymbol{I}, \ \boldsymbol{N}2 = \boldsymbol{I} - \bar{\boldsymbol{J}}1^{+}\bar{\boldsymbol{J}}1 \tag{51d}$$

$$\begin{aligned} \bar{\boldsymbol{J}}1 &= \boldsymbol{J}1\boldsymbol{N}1 = \boldsymbol{J}1, \ \bar{\boldsymbol{J}}2 = \boldsymbol{J}2\boldsymbol{N}2 \\ &= \boldsymbol{J}2(\boldsymbol{I} - \boldsymbol{J}1^{+}\boldsymbol{J}1) \end{aligned} \tag{51e}$$

$$\boldsymbol{\Gamma} = [\bar{\boldsymbol{J}}1^\top \ \bar{\boldsymbol{J}}2^\top]^\top \tag{51f}$$

$$\begin{aligned} \boldsymbol{\Gamma}^\dagger &= [\bar{\boldsymbol{J}}1^{+} \ \bar{\boldsymbol{J}}2^{+}] \\ &= [\bar{\boldsymbol{J}}1^{\mathrm{T}}(\bar{\boldsymbol{J}}1\bar{\boldsymbol{J}}1^{\mathrm{T}})^{-1} \ \bar{\boldsymbol{J}}2^{\mathrm{T}}(\bar{\boldsymbol{J}}2\bar{\boldsymbol{J}}2^{\mathrm{T}})^{-1}]. \end{aligned} \tag{51g}$$

The mass matrix $\boldsymbol{M}$ and the gain matrices were set as follows

$$\begin{aligned} \boldsymbol{M} = \mathrm{diag}(&3.8\times10^{-3}\ \mathrm{kgm}^2, \ 3.8\times10^{-3}\ \mathrm{kgm}^2, \\ &0.16\ \mathrm{kg}, \ 3.8\times10^{-3}\ \mathrm{kgm}^2, \\ &3.8\times10^{-3}\ \mathrm{kgm}^2, \ 0.16\ \mathrm{kg}) \end{aligned} \tag{52a}$$

$$\begin{aligned} \boldsymbol{K}\mathrm{pp} = \mathrm{diag}(&6400\ \mathrm{Nm/rad}, \ 6400\ \mathrm{Nm/rad}, \\ &100\ \mathrm{N/m}, \ 6400\ \mathrm{Nm/rad}, \\ &6400\ \mathrm{Nm/rad}, \ 900\ \mathrm{N/m}) \end{aligned} \tag{52b}$$

$$\begin{aligned} \boldsymbol{K}\mathrm{ap} = \mathrm{diag}(&6400\ \mathrm{Nm/rad}, \ 6400\ \mathrm{Nm/rad}, \\ &100\ \mathrm{N/m}, \ 900\ \mathrm{Nm/rad}, \\ &900\ \mathrm{Nm/rad}, \ 400\ \mathrm{N/m}) \end{aligned} \tag{52c}$$

$$\begin{aligned} \boldsymbol{K}\mathrm{pv} = \mathrm{diag}(&480\ \mathrm{Nm\cdot s/rad}, \ 480\ \mathrm{Nm\cdot s/rad}, \\ &80\ \mathrm{Ns/m}, \ 480\ \mathrm{Nm\cdot s/rad}, \\ &480\ \mathrm{Nm\cdot s/rad}, \ 100\ \mathrm{Ns/m}) \end{aligned} \tag{52d}$$

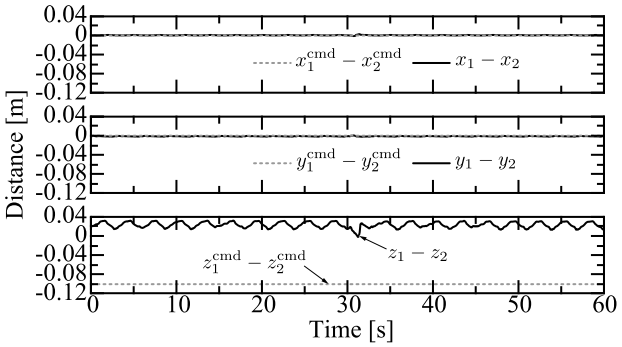

(a) First-priority task.

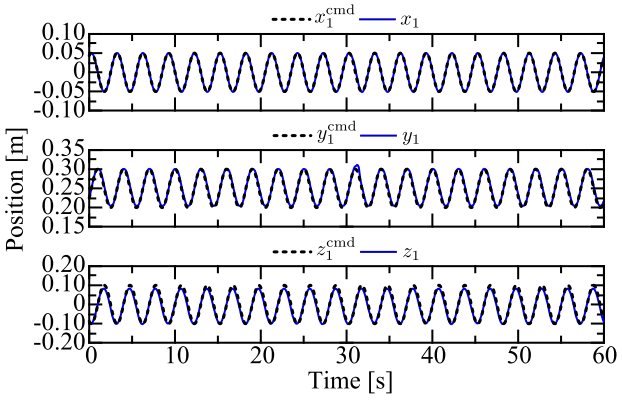

(b) Second-priority task.

FIGURE 5. Experimental results with the conventional method.

$$\begin{aligned} \boldsymbol{K}\mathrm{av} = \mathrm{diag}(&480\ \mathrm{Nm\cdot s/rad}, \ 480\ \mathrm{Nm\cdot s/rad}, \\ &80\ \mathrm{Ns/m}, \ 450\ \mathrm{Nm\cdot s/rad}, \\ &450\ \mathrm{Nm\cdot s/rad}, \ 40\ \mathrm{Ns/m}), \end{aligned} \tag{52e}$$

which satisfy that the matrix $\boldsymbol{A} + p2\boldsymbol{A}\mathrm{p}$ is Hurwitz and the global asymptotic stability with Theorem 1. The quasi-periodic and quasi-aperiodic commands were

$$z1^{\mathrm{cmd}} = [\,0\ \mathrm{m}\ \ 0\ \mathrm{m}\ \ -0.1\ \mathrm{m}\,]^\top \tag{53a}$$

$$z2\mathrm{p}^{\mathrm{cmd}} = \begin{bmatrix} -0.05\sin\dfrac{2\pi}{3}t\ \mathrm{m} \\ 0.3 - 0.05\left(1 - \cos\dfrac{2\pi}{3}t\right)\ \mathrm{m} \\ 0.1\sin\dfrac{2\pi}{3}t\ \mathrm{m} \end{bmatrix} \tag{53b}$$

$$z2\mathrm{a}^{\mathrm{cmd}} = \boldsymbol{0}. \tag{53c}$$

Before the activation of the proposed method ($t < 0$ s), the classical priority control without the periodic/aperiodic separation control was conducted with the first-priority grasping task and the second-priority quasi-periodic task only for the initialization of the PASF. After initializing the PASF, the proposed method was activated. For the PASF, the separation frequency was set to $\rho = 0.01$ rad/s.

The experiments compared the proposed method with the conventional priority control [5]. The conventional method prioritized tasks on the basis of the null space projection in

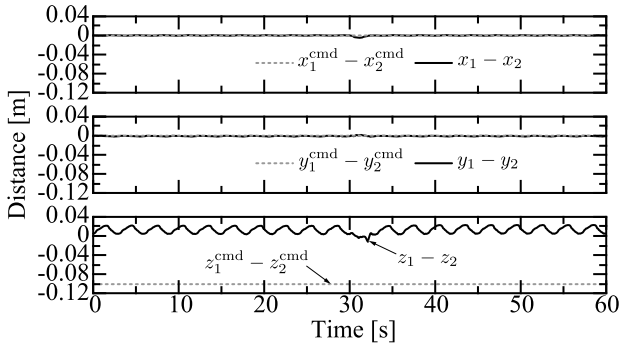

(a) First-priority task.

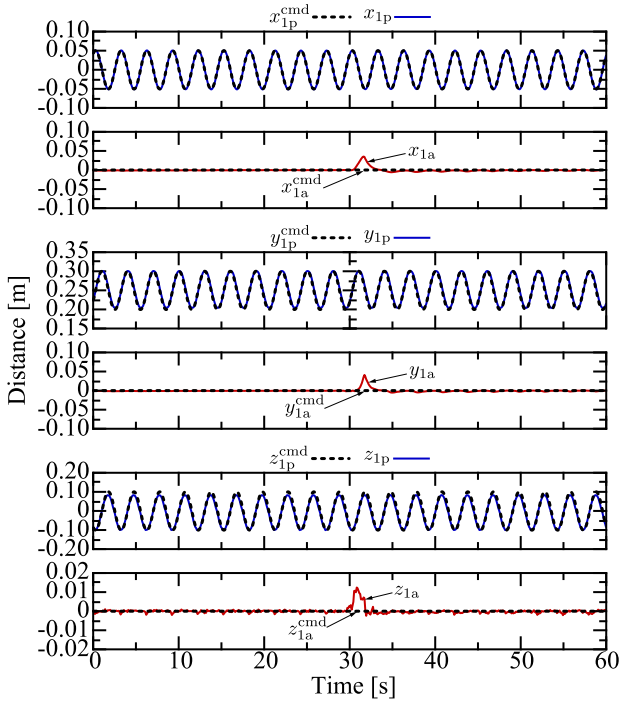

(b) Second-priority task.

FIGURE 6. Experimental results with the proposed method.

the same manner as the proposed method, while it did not realize the quasi-periodic and quasi-aperiodic tasks. Hence, in the experiment, the conventional method realized the task assigned to the proposed method as the quasi-periodic task in the second-priority level. In the first-priority level, the conventional method realized the same task as that of the proposed method.

The experimental results with the conventional method are shown in Figure 5. In the first-priority task shown in Figure 5(a), the displacement between the upper and lower robots in x and y directions was almost zero, and the z direction was impedance controlled for grasping a ball. The error between the command $z1^{\mathrm{cmd}} - z2^{\mathrm{cmd}}$ and response $z1 - z2$ was caused by grasping the ball and corresponds to the size of the ball. In the second-priority task shown in Figure 5(b), the position responses $x1$, $y1$, and $z1$ followed the commands $x1^{\mathrm{cmd}}$, $y1^{\mathrm{cmd}}$, and $z1^{\mathrm{cmd}}$. Thus, the conventional method performed the six tasks including the two first-priority synchronizations of the upper and lower robots in x and y directions, one first-priority impedance controlled ball grasping in z direction, and three second-priority positionings of the upper robot in x, y, and z directions.

The experimental results with the proposed method are shown in Figure 6. The proposed method achieved the prioritization of the first-priority task of Figure 6(a) and the second-priority task of Figure 6(b) on the basis of the torque computation (23) and achieved the quasi-periodic and quasi-aperiodic tasks as Figure 6(b) on the basis of the separation control (29). Figure 6(a) shows similar results to those of Figure 5(a) because they used the same control in the first-priority level. In the second-priority level, quasi-periodic moving task and quasi-aperiodic adaption task were conducted, where the quasi-periodic position responses tracked their commands and the quasi-aperiodic position moved to be adaptive against the experimenter's contact in 30–35 s, as shown in Figure 6(b). Thus, the proposed method performed the nine tasks including the two first-priority synchronizations of the upper and lower robots in x and y directions, one first-priority impedance controlled ball grasping in z direction, three second-priority quasi-periodic positioning of the upper robot in x, y, and z directions, and three second-priority quasi-aperiodic impedance controlled adaptation task in x, y, and z directions. Therefore, compared to the conventional method, the proposed method achieved to increase the number of realizable tasks from six to nine.

VI. CONCLUSION

This paper proposed the integrated control of the priority control and periodic/aperiodic separation control. The proposed method can realize prioritized and separated quasi-periodic and quasi-aperiodic tasks, where the lower-priority quasi-periodic and quasi-aperiodic tasks are modified not to disturb higher-priority tasks. The global asymptotic stability was proved on the basis of the Lyapunov function, and the experiments comparatively validated the proposed method increased the number of realizable tasks with first-priority grasping, second-priority quasi-periodic moving, and second-priority quasi-aperiodic adaptation tasks.

REFERENCES

[1] A. Karami, H. Sadeghian, M. Keshmiri, and G. Oriolo, "Force, orientation and position control in redundant manipulators in prioritized scheme with null space compliance," *Control Eng. Pract.*, vol. 85, pp. 23–33, Apr. 2019.

[2] C. Ott, A. Dietrich, and A. Albu-Schäffer, "Prioritized multi-task compliance control of redundant manipulators," *Automatica*, vol. 53, pp. 416–423, Mar. 2015.

[3] H. Sadeghian, L. Villani, M. Keshmiri, and B. Siciliano, "Multi-priority control in redundant robotic systems," in *Proc. IEEE/RSJ Int. Conf. Intell. Robots Syst.*, Sep. 2011, pp. 3752–3757.

[4] D. Ortenzi, R. Muthusamy, A. Freddi, A. Monteriù, and V. Kyrki, "Dual-arm cooperative manipulation under joint limit constraints," *Robot. Auto. Syst.*, vol. 99, pp. 110–120, Jan. 2018.

[5] J. Obregón-Flores, G. Arechavaleta, H. M. Becerra, and A. Morales-Díaz, "Predefined-time robust hierarchical inverse dynamics on torque-controlled redundant manipulators," *IEEE Trans. Robot.*, vol. 37, no. 3, pp. 962–978, Jun. 2021.

[6] A. Dietrich and C. Ott, "Hierarchical impedance-based tracking control of kinematically redundant robots," *IEEE Trans. Robot.*, vol. 36, no. 1, pp. 204–221, Feb. 2020.
[7] A. Dietrich, C. Ott, and A. Albu-Schäffer, "An overview of null space projections for redundant, torque-controlled robots," *Int. J. Robot. Res.*, vol. 34, no. 11, pp. 1385–1400, Mar. 2015.
[8] A. Karami, H. Sadeghian, M. Keshmiri, and G. Oriolo, "Hierarchical tracking task control in redundant manipulators with compliance control in the null-space," *Mechatronics*, vol. 55, pp. 171–179, Nov. 2018.
[9] G. Antonelli, "Stability analysis for prioritized closed-loop inverse kinematic algorithms for redundant robotic systems," in *Proc. IEEE Int. Conf. Robot. Autom.*, May 2008, pp. 1993–1998.
[10] H. Xing, A. Torabi, L. Ding, H. Gao, Z. Deng, V. K. Mushahwar, and M. Tavakoli, "An admittance-controlled wheeled mobile manipulator for mobility assistance: Human–robot interaction estimation and redundancy resolution for enhanced force exertion ability," *Mechatronics*, vol. 74, Apr. 2021, Art. no. 102497.
[11] A. Escande, N. Mansard, and P.-B. Wieber, "Hierarchical quadratic programming: Fast online humanoid-robot motion generation," *Int. J. Robot. Res.*, vol. 33, no. 7, pp. 1006–1028, Jun. 2014.
[12] S. Kim, K. Jang, S. Park, Y. Lee, S. Y. Lee, and J. Park, "Continuous task transition approach for robot controller based on hierarchical quadratic programming," *IEEE Robot. Autom. Lett.*, vol. 4, no. 2, pp. 1603–1610, Jan. 2019.
[13] H. M. Pérez-Villeda, G. Arechavaleta, and A. Morales-Díaz, "Multi-vehicle coordination based on hierarchical quadratic programming," *Control Eng. Pract.*, vol. 94, Jan. 2020, Art. no. 104206.
[14] F. Tassi, E. De Momi, and A. Ajoudani, "An adaptive compliance hierarchical quadratic programming controller for ergonomic human–robot collaboration," *Robot. Comput.-Integr. Manuf.*, vol. 78, Dec. 2022, Art. no. 102381.
[15] K. Bouyarmane and A. Kheddar, "Using a multi-objective controller to synthesize simulated humanoid robot motion with changing contact configurations," in *Proc. IEEE/RSJ Int. Conf. Intell. Robots Syst.*, Sep. 2011, pp. 4414–4419.
[16] J. Salini, V. Padois, and P. Bidaud, "Synthesis of complex humanoid whole-body behavior: A focus on sequencing and tasks transitions," in *Proc. IEEE Int. Conf. Robot. Autom.*, May 2011, pp. 1283–1290.
[17] H. Muramatsu, "Separation and estimation of periodic/aperiodic state," *Automatica*, vol. 140, Jun. 2022, Art. no. 110263.
[18] H. Muramatsu and S. Katsura, "Periodic/aperiodic motion control using periodic/aperiodic separation filter," *IEEE Trans. Ind. Electron.*, vol. 67, no. 9, pp. 7649–7658, Sep. 2020.
[19] H. Muramatsu and S. Katsura, "Separated periodic/aperiodic state feedback control using periodic/aperiodic separation filter based on lifting," *Automatica*, vol. 101, pp. 458–466, Mar. 2019.
[20] D. Aslan and Y. Altintas, "On-line chatter detection in milling using drive motor current commands extracted from CNC," *Int. J. Mach. Tools Manuf.*, vol. 132, pp. 64–80, Sep. 2018.
[21] Y. Sugiura, A. Kawamura, and N. Aikawa, "A comb filter with adaptive notch bandwidth for periodic noise reduction," in *Proc. 9th Int. Conf. Inf., Commun. Signal Process.*, Dec. 2013, pp. 1–4.
[22] J. Liu and N. F. Declercq, "Pulsed ultrasonic comb filtering effect and its applications in the measurement of sound velocity and thickness of thin plates," *Ultrasonics*, vol. 75, pp. 199–208, Mar. 2017.
[23] H. Muramatsu and S. Katsura, "An adaptive periodic-disturbance observer for periodic-disturbance suppression," *IEEE Trans. Ind. Informat.*, vol. 14, no. 10, pp. 4446–4456, Oct. 2018.
[24] H. Muramatsu and S. Katsura, "An enhanced periodic-disturbance observer for improving aperiodic-disturbance suppression performance," *IEEJ J. Ind. Appl.*, vol. 8, no. 2, pp. 177–184, Mar. 2019.
[25] H. Muramatsu and S. Yamato, "Harmonics elimination by periodic/aperiodic separation filter for chatter detection," *Trans. Inst. Syst., Control Inf. Eng.*, vol. 36, no. 3, pp. 64–71, Mar. 2023.

HISAYOSHI MURAMATSU (Member, IEEE) received the B.E. degree in system design engineering and the M.E. and Ph.D. degrees in integrated design engineering from Keio University, Yokohama, Japan, in 2016, 2017, and 2020, respectively. From 2019 to 2020, he was a Research Fellow with the Japan Society for the Promotion of Science. Since 2020, he has been with Hiroshima University, Higashihiroshima, Japan. His research interests include motion control, robotics, mechatronics, and control engineering.

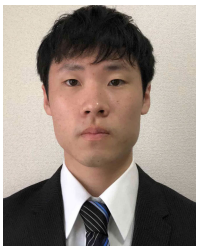

MASAKI HINO received the B.E. degree in mechanical systems and the M.E. degree in mechanical engineering from Hiroshima University, Higashihiroshima, Japan, in 2020 and 2022, respectively. Since 2022, he has been with the Technical Division, Satake Corporation, Higashihiroshima.